AAPS PharmSciTech, Vol. 9, No. 4, December 2008 (© 2008)
DOI: 10.1208/s12249-008-9145-6

Research Article

Monitoring Granulation Rate Processes Using Three PAT Tools in a Pilot-Scale Fluidized Bed

Ai Tee Tok,[1] Xueping Goh,[1] Wai Kiong Ng,[1,3] and Reginald B. H. Tan[1,2]

Received 31 March 2008; accepted 2 September 2008; published online 11 October 2008

Abstract. The purpose of this research was to analyze and compare the responses of three Process Analytical Technology (PAT) techniques applied simultaneously to monitor a pilot-scale fluidized bed granulation process. Real-time measurements using focused beam reflectance measurement (Lasentec FBRM) and near-infra red spectroscopy (Bruker NIR) were taken by inserting in-line probes into the fluidized bed. Non-intrusive acoustic emission measurements (Physical Acoustic AE) were performed by attaching piezoelectric sensors on the external wall of the fluidized bed. Powder samples were collected at regular intervals during the granulation process and characterized offline using laser diffraction, scanning electron microscopy, stereo-optical microscopy and loss on drying method. PAT data comprising chord length distribution and chord count (from FBRM), absorption spectra (from NIR) and average signal levels and counts (from AE) were compared with the particle properties measured using offline samples. All three PAT techniques were able to detect the three granulation regimes or rate processes (wetting and nucleation, consolidation and growth, breakage) to varying degrees of sensitivity. Being dependent on optical signals, the sensitivities of the FBRM and NIR techniques were susceptible to fouling on probe windows. The AE technique was sensitive to background fluidizing air flows and external interferences. The sensitivity, strengths and weaknesses of the PAT techniques examined may facilitate the selection of suitable PAT tools for process development and scale-up studies.

KEY WORDS: acoustic emission; FBRM; granulation; near-infra red; PAT.

INTRODUCTION

Fluidized bed granulation is widely applied in pharmaceutical secondary manufacturing as a one-pot system, which integrates wetting, drying, mixing, particle size enlargement and particle shaping into a single unit operation. It improves flow properties, reduces dustiness, increases bulk density, and brings about co-mixing (1). As several processes are involved in this system, numerous process variables such as air flow rate, temperature, humidity of inlet air, binder addition rate, and droplet size of liquid binder are known to affect the quality of the final granules (2). Being such a complex process, it is difficult to scale-up based on the process variables alone (3). Even when pilot-scale testing does occur, there is still a significant failure rate during scale-up to industrial production (1). Recently, the US Food and Drug Administration (FDA) has encouraged the use of on- or in-line process analyzers or Process Analytical Technology (PAT) to collect data of intermediate or product properties in real-time. On-line measurement requires the sample to be diverted from the manufacturing process for analysis whereas no sample is removed from the process stream for in-line measurement. Such techniques can potentially provide valuable insight and understanding for process optimization, scale-up and technology transfer (4) but are still not well established in secondary manufacturing yet.

Historically, human hearing has served as an early form of real-time process analyzer. Experienced operators in the pharmaceutical industry were able to monitor a granulation process by listening to the acoustic signals emitted and determine the process end-point. However, transferring such know-how to new operators has been difficult due to the lack of scientific understanding. To decipher the science behind this know-how, acoustic emission (AE) measurement has been found to be a useful tool as it can detect acoustic signals both audible and beyond the frequency range of the human hearing which is 20 Hz to 20 kHz (5). Past studies reported that a granulation process typically emits significant acoustic signals in the range of 20 to 350 kHz (6,7). Tsujimoto *et al.* (7) categorized the basic sources of acoustic signals from fluidized beds into (1) particle–particle or particle–chamber collision (impact sounds), (2) particle–particle or particle–chamber friction (friction sound) and (3) air turbulence in particle beds (aerodynamic sound). Tsuijimoto *et al.* (7) found that the mean AE amplitude correlated well with dimensionless excess gas velocity, dimensionless bed height and particle

[1] Crystallisation and Particle Sciences, Institute of Chemical and Engineering Sciences, Agency for Science Technology and Research (A*STAR), 1 Pesek Road, Jurong Island, Singapore 627833, Singapore.
[2] Department of Chemical and Biomolecular Engineering, The National University of Singapore, 4 Engineering Drive 4, Singapore 117576, Singapore.
[3] To whom correspondence should be addressed. (e-mail: ng_wai_kiong@ices.a-star.edu.sg)

size. Halstensen *et al.* (8) demonstrated the feasibility of using acoustic chemometrics measurements to predict fluidization air flow, reflux of fines, granule moisture content and general process states in a semi-industrial pilot plant for urea production. Whitaker *et al.* (6) reported correlations between acoustics emission signals and particle size, powder flow and compression properties in a high shear granulation process. There were also other reports on the use of acoustic emission to monitor granulation and coating processes (9).

The use of an image probe for real-time monitoring of particle size distribution and morphology in a fluidized bed granulator was pioneered by Watano and Miyanami (10). More recently, commercial in-line particle size analyzers based on laser backscattering have emerged in the market. Numerous studies on the use of laser backscattering, also called the focused beam reflectance measurement (FBRM), were based on modeling or the restoration of particle size through the measurement of chord length distribution of particles suspended in a liquid medium, particularly in crystallization processes (11–13). The Lasentec FBRM instrument uses low-level laser light to measure the particle chord length. A laser beam is projected through the sapphire window of the FBRM probe, which is inserted into a suspension or powder bed. The laser beam is focused just outside the window and is moved so that it follows a path around the circumference of the probe window. As particles pass by the window surface, the focused beam will intersect the edge of a particle. The backscatter of the laser beam by the particle is collected by the FBRM optics and converted to size measurement (chord length) of the particle (14). However, there are currently few reports on using this technique to monitor the granulation process. They are found in presentation materials prepared by two leading instrument suppliers under the trade names, Lasentec and Parsum.

The use of in-line or on-line near-infra red spectroscopy (NIR) has been reported to monitor changes in granule properties during fluidization. Simultaneous real-time monitoring of particle size and moisture content using in-line NIR in a lab-scale fluidized bed granulator was demonstrated by Finlay *et al.* (15). Rantanen *et al.* (16) investigated the effect of particle size of glass beads on NIR spectra. A simple logarithmic calibration model has also been developed to correlate the moisture content with NIR spectral response (17). Frake *et al.* (18) reported a linear relationship between the second derivative absorbance changes at wavenumber of 5,175 cm^{-1} (or wavelength of 1,932 nm) and moisture content. Models have been developed to predict particle size and moisture content using principal component analysis or partial least square regression of NIR data (19).

Though there are reports on the use of individual PAT techniques in fluidized bed granulation, no study has been conducted to compare the results of several PAT tools within the same process to the best of the authors' knowledge. Therefore, the objective of this paper was to apply two in-line (FBRM and NIR) and one non-intrusive (AE) PAT techniques simultaneously in a pilot-scale top spray fluidized bed granulator (bottom internal diameter 0.3 m, height 0.6 m) to monitor the progress of the granulation process. Non-intrusive refers to having no physical contact between the analytical probe and the process stream. The signals captured by each technique were compared against the occurrence of the different regimes or granulation rate processes (wetting and nucleation, consolidation and growth, breakage) as classified by Ennis and Lister (20). The occurrence of each rate process was determined from offline analysis of samples using Malvern laser diffraction (particle size distribution), scanning electron and optical microscopy (morphology). These rate processes are at the heart of granulation and the inter-play between these processes determine the final granule properties, such as granule-size distribution, porosity as well as other key product attributes. For instance, if small uniformly sized granules are desired, the ideal region of operation is in the nucleation or the induction-growth regime. However, if relatively coarse granules are required, the steady-growth regime is preferred as this minimizes the operational time and the final size can be tuned through binder content and residence time (21). An appropriate PAT technique can potentially monitor which granulation rate process is dominating and provide early warnings of any deviation from the desired intermediate or product quality. This would allow timely adjustment of the relevant process variables, assure good product quality and prevent critical shutdown situations (e.g., over-drying, defluidization).

MATERIALS AND METHODS

Materials

Each granulation batch consists of 1.2 kg powder mixture of alpha lactose monohydrate and microcrystalline cellulose (MCC, grade PH-101; Sigma Aldrich) in weight ratio of 9:1. Lactose and MCC were chosen as they are common excipients found in the pharmaceutical industry, which are widely used for direct compression and wet granulation. With particle size d_{50} of 53 μm and bulk density of 0.5 g/cm^3, this mixture falls into Geldart class A (22), which typically fluidizes smoothly at low gas velocities and with small bubbles at higher velocities (23). The liquid binder solution comprises 2.5 wt.% of polyvinylpyrrolidone (PVP, grade K-30; Fluka) dissolved in deionized water.

Methods

Fluidized Bed Granulation

Figure 1 shows a schematic diagram of the pilot-scale fluidized bed granulator showing the positions of each PAT probe. The bed was designed with a bottom internal diameter (i.d.) of 0.3 m to ensure that bubbling rather than slugging fluidization takes place, which was recommended as minimum i.d. by Ennis and Lister (20). The acoustic emission sensors were attached onto the external walls of the fluidized bed while the FBRM and NIR probes were inserted into the fluidized bed at an inclined angle of 30° and at a depth of 0.02 m above the center of the stainless steel sintered distributor plate. Dry compressed air with a relative humidity of less than 2% and at 25°C (FESTO flowmeter, model MS6-SFE-F5-P2U-M12) was used as the fluidizing medium. The fluidizing air flow rate was steadily increased from 1,000 to 1,550 L/min during the granulation process as the granules grow in size, in order to maintain them in a fluidized state. The binder solution was supplied by a peristaltic pump at 3 to 4 g/min through an atomizer (Schlick, model 942/7-1) at

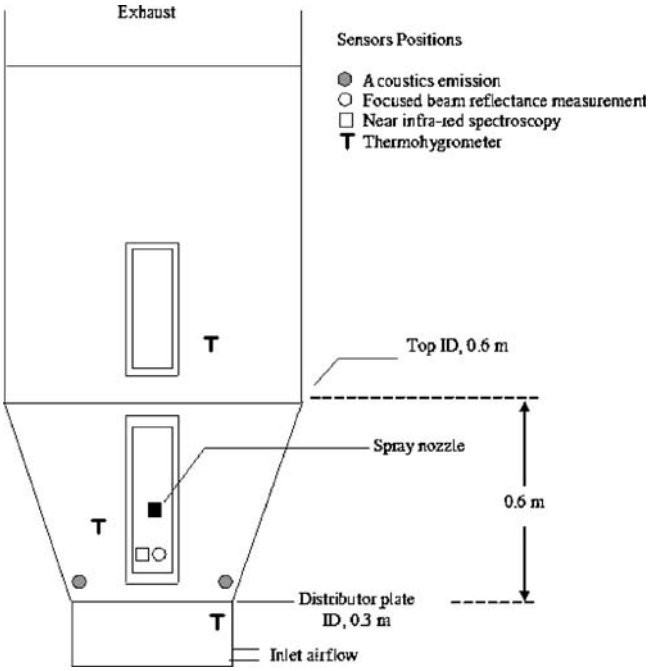

Fig. 1. Schematic diagram of pilot-scale fluidized bed granulator

pressure of 0.3 bar. 10 g of samples were collected from the centre of the fluidized bed after the first 10 min and subsequently every 20 min for the entire granulation duration of 130 min. No liquid spray was applied during the last 10 min to serve as a drying stage to simulate process upsets such as over drying or clogging of spray nozzle.

PAT In-line Techniques

The operating conditions of the three PAT in-line techniques are described below. Focused beam reflectance measurement (FBRM, Lasentec model D600P, USA) measures the chord length distribution (CLD) of the particles and chord counts per s at every min interval during granulation. The focal point of the measurement was set at +100 μm from the probe window, so as to avoid distorted readings arising from fines coated onto the window at the initial stage of granulation. Anti-static spray (Electrolube ASA, UK) was applied onto the surface of the probe window before the experimental run. Near-infra red spectroscopy (NIR) is a non destructive analytical technique that measures the absorption intensity over the near-infra red electromagnetic spectrum from wavenumber of 12,820 to 3,959 cm^{-1} as defined by ASTM standards. NIR process analyzer (Bruker, model Matrix-F, Germany) equipped with an in-line probe was used to measure absorption intensity over wavenumber of 12,000 to 4,000 cm^{-1} by the fluidized particles. Similarly, anti-static spray was applied onto the window of the NIR probe to reduce the coating of fines. Two acoustic emission (AE) piezoelectric sensors (Physical Acoustics, models R6I and R15I, USA) were attached onto the external walls of the granulator using grease as the coupling agent. The operating frequency range of R6I is from 40 to 100 kHz with main resonance at 50 kHz while the operating frequency range of R15I is from 70 to 200 kHz with main resonance at 125 kHz. In the region from 50 to 450 kHz, attenuation is high and sound propagates only relatively short distances. Measurement in this region offers the advantage that processes can be monitored with little interference from extraneous noise (6). The AE technique measures the average signal level (ASL) based on a time constant of 500 ms and counts per AE duration.

Offline Techniques

The particle size distribution (PSD) of the samples obtained was measured by laser diffraction (Malvern, model Scirocco 2000) using dry dispersion method at pressure of 0.1 bar and measurement duration of 10 s. Low dispersing

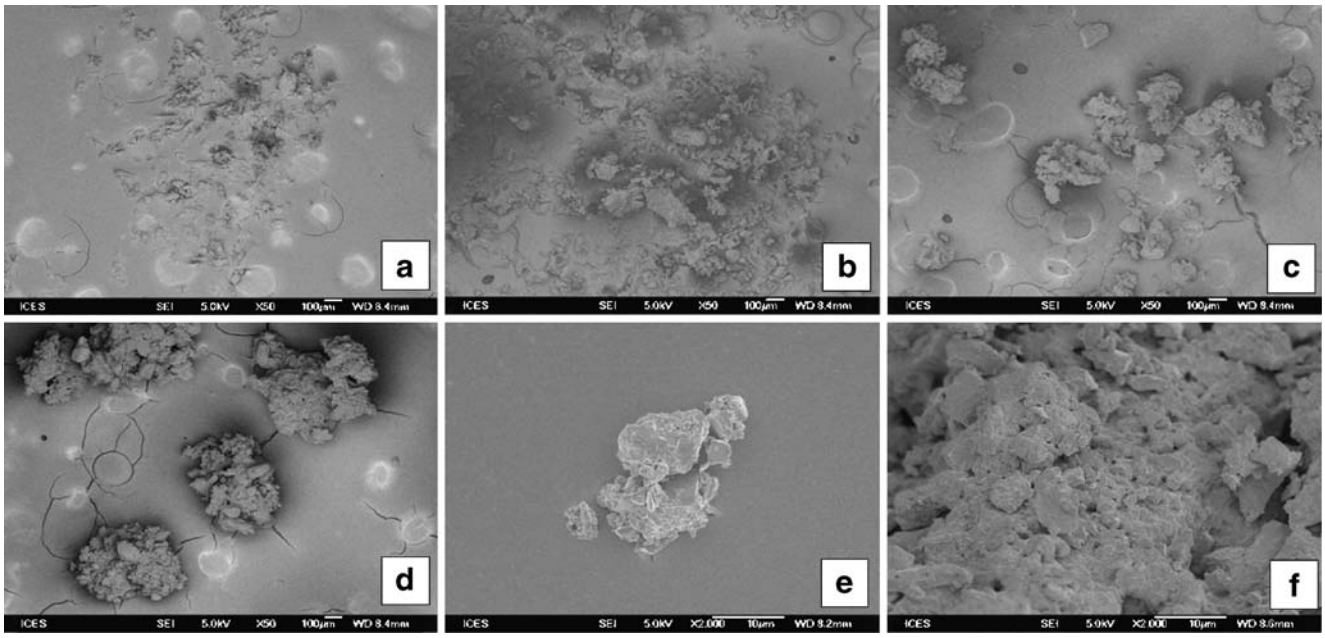

Fig. 2. SEM photomicrographs at ×50 magnification **a** before granulation, **b** 20 min granulation, **c** 60 min granulation, **d** 120 min granulation, at ×2,000 magnification **e** before granulation **f** 120 min granulation

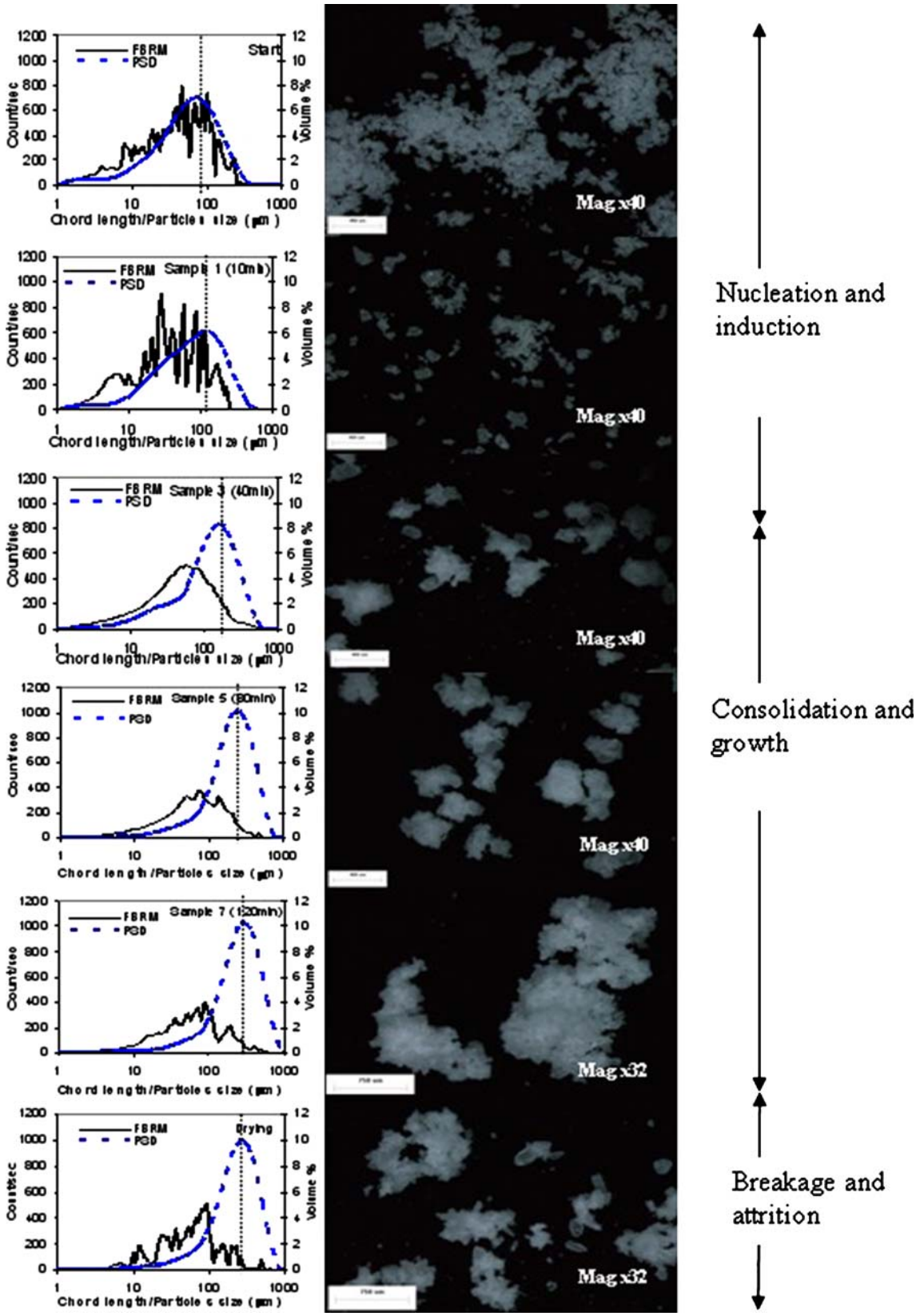

Fig. 3. FBRM CLD (*solid line*) with PSD by laser diffraction (*dotted line*) and corresponding photomicrographs at different granulation time

pressure was selected so as to minimize breakage of granules. Each measurement was done in triplicate. The laser diffraction technique was needed because the particle chord length data from FBRM were not directly transferable to PSD (14). The sample moisture content was analyzed using loss on drying (LOD) method. Approximately 1 g was measured

before and after drying in an oven at 110°C over 18 h. Surface morphology and size of the samples were examined using a stereomicroscope (Leica, model MZ16) equipped with a digital camera (model DFC320) and process software (Image.Pro MDA 6.0) at magnification of ×40 or ×32 as well as using a scanning electron microscope (SEM, JEOL, model JSM-6700F) at a voltage of 5 kV and magnification of ×50 and ×2,000. Prior SEM analysis, the samples were sputtered with a thin layer of gold (Edwards sputter coater, UK).

RESULTS AND DISCUSSION

Offline Granule Characterization

As shown in Figs. 2 and 3, optical and SEM photomicrographs of samples taken at various stages of granulation compares well with the occurrence of the three granulation rate processes (wetting and nucleation, consolidation and growth, breakage) classified by Ennis and Lister or Iveson *et al* (1,20) as shown in Fig. 4. The PSD and the moisture content of the samples collected are given in Table I. During the initial 20 min, the particle size d_{50} increased at a rate of 1.1 μm/min from 52.9 to 74.6 μm, which was followed by a more rapid growth rate of 2.0 μm/min between 20 and 80 min. In the first 20 min, the growth behavior appeared to fall into the nucleation or induction-growth regime, whereby the granules consolidate over an induction period before steady and faster growth can follow. This occurrence is typical for granulation systems with fine powders, viscous liquid binder and relatively low level of agitation intensity like the current system. The low moisture content of 3 to 4.5 wt.% may have also contributed to the occurrence of a nucleation or induction period, whereby sufficient deformation of granules was expected before steady growth could take place (21). The PSD results were supported by optical and SEM photomicrographs showing that the samples taken in the first 20 min were mainly discrete particles with well-defined edges. Subsequently, fines disappeared were not seen in the images due to the agglomeration process leading to particle growth. As shown in Fig. 3f, smoothing of the particle edges and fusion of fines revealed that dissolution, agglomeration and drying had taken place. From 80 to 120 min, the particle size d_{50} decreased from 197 to 190.4 μm and then increased again to 240.5 μm, giving an average growth rate of 1 μm/min. The results suggested that the steady-growth phase has ended and the decrease in particle growth rate was probably due to a balance of aggregation and attrition or breakage processes. During the last 10 min, the decrease in particle size from 240.5 to 220.3 μm and the presence of fines shown in Fig. 4 were clearly due to the breakage and attrition of granules. The breakage process could be attributed to the drying of the granules in the absence of the liquid binder, which was seen from the decrease in moisture content from 3.9 to 3.4 wt.% in Table I. Throughout the granulation process, as the moisture content remained low and consistent between 3.4 and 4.5 wt.%, the influence of moisture content on PAT data was not taken into account for this study.

Table I. Particle Size and Moisture Content Results

Sampling time	Particle size [μm] d_{50}	Moisture content [%]
Before granulation	52.9	3.9
10 min	68.7	3.6
20 min	74.6	4.0
40 min	116.2	4.2
60 min	136.1	3.8
80 min	197.0	4.4
100 min	190.4	3.6
120 min	240.5	3.9
130 min	220.3	3.4

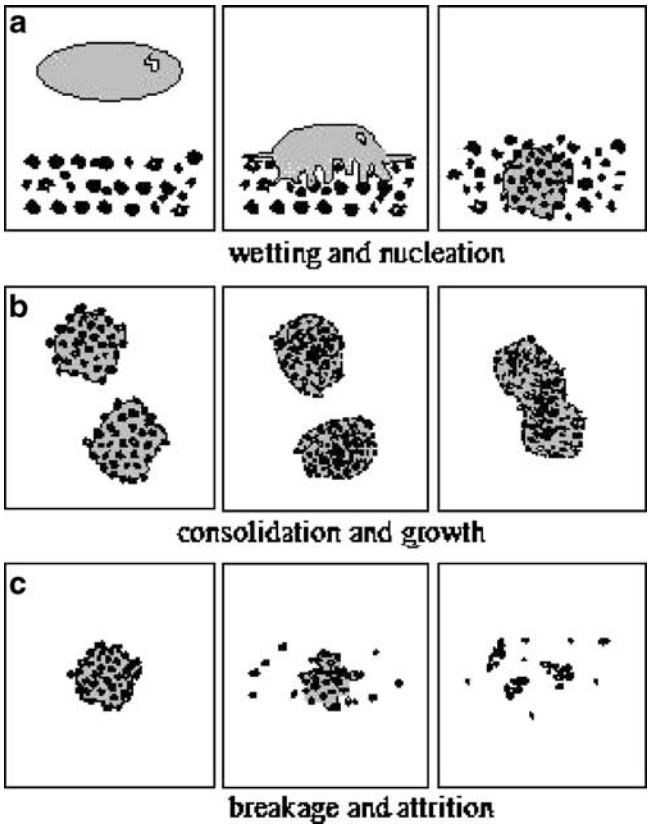

Fig. 4. Rate processes in fluidized bed granulation, adapted from Iveson *et al.* (1)

FBRM Results

The measured particle chord length distribution (CLD) and chord count/s are plotted against granulation time together with PSD of samples collected in Fig. 5.

Square-weighted CLD was selected as it was reported to give the best agreement with the conventional laser diffraction particle size distribution for suspensions of various particle sizes (24). During the first 10 min, the decrease in chord length with an accompanying increase in chord count suggested an induction period where the breaking up of physical aggregates of particles took place. From 10 to 80 min, the steady increase in chord length from 68.7 to 197 μm and a decline in chord count/s showed the occurrence of a steady-growth phase, which tallied with the earlier reported steady particle size growth. Subsequently, the chord length data became more scattered and showed an increase from 100 to 120 min, which corresponded well with particle size data. Beyond 80 min, the scattering of

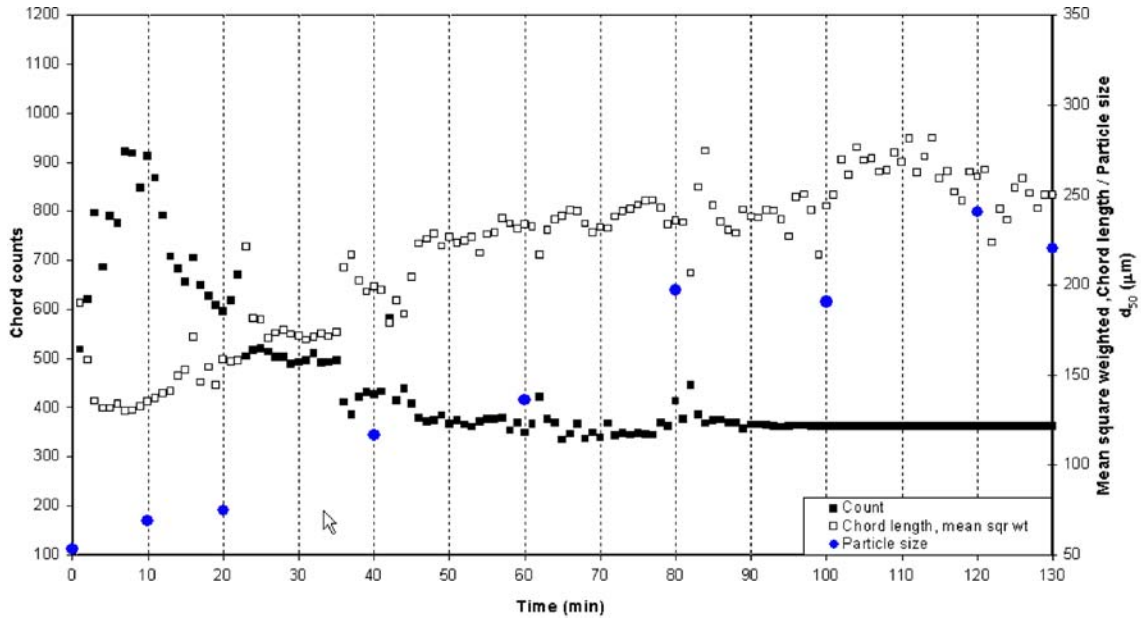

Fig. 5. Comparison of FBRM data: mean square weighted chord length and counts with particle size d_{50} by laser diffraction

chord length distribution (CLD) data was also seen in Fig. 5. Worlitschek *et al.* (13) observed the scattering of CLD data of particles suspended in a liquid medium and attributed it to low chord counts leading to statistical errors. In the current process, the scattering data was likely caused by granule breakage or attrition leading to the generation of fines. The rapid change in the particle count and size could have led to similar statistical errors. The scattered CLD plots were seen both at the beginning and end of the granulation process where significant fines were present. During the last 10 min, the decrease in chord length in Fig. 5 also corresponded with the reduction in particle size.

One problem encountered when using the FBRM is the fouling of the optical probe during the start of granulation, which has previously been reported for suspensions of various particle sizes (24). The probe window was partially coated by a layer of fines, which initially distorted the chord length measurements. This problem was minimized by increasing the focal point of the measurement from the normal setting of +20 to +100 µm. The influence of the focal point on CLD has also been reported by Worlitschek and Mazzotti (25).

NIR Spectra

Figure 6 shows a plot of NIR spectra at various granulation times. The spectra showed a shift in baseline with increasing granulation time. To compare the baseline shift with changes in

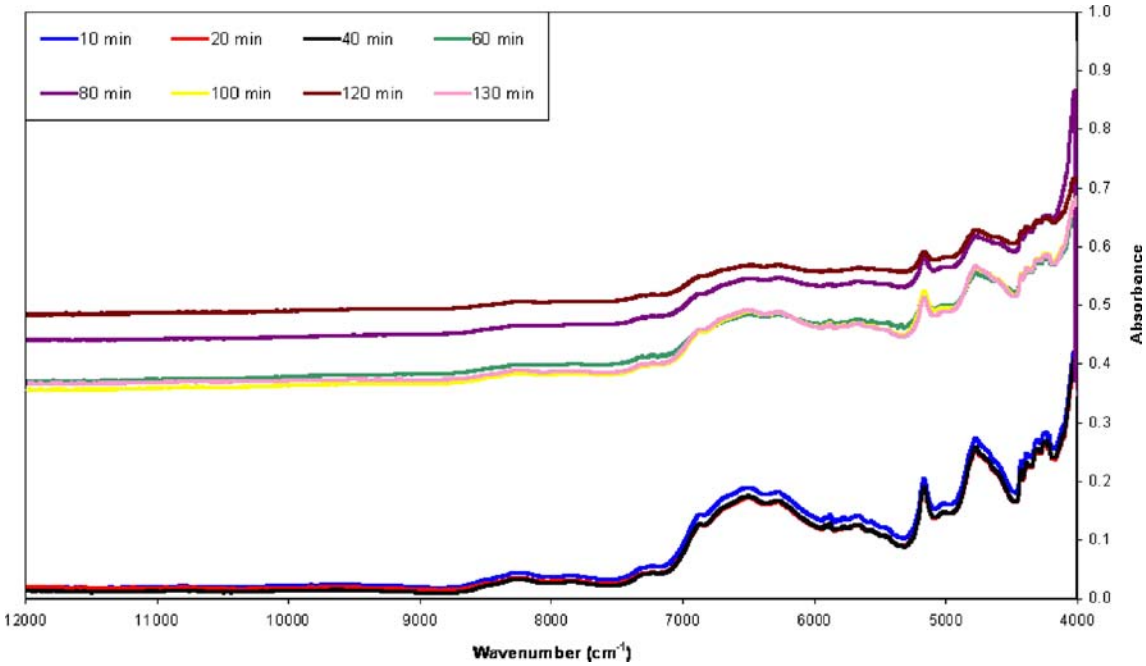

Fig. 6. NIR spectra over granulation time

particle size, the absorption intensity or absorbance at selected wavenumber of 10,000 cm^{-1} was plotted together with particle size d_{50} against granulation time and shown in Fig. 7. The measured absorbance was low at around 0.02 units for the first 50 min and increased abruptly to 0.38 units at 60 min. The sudden increase at 50 min did not tally with the onset of steady-growth phase at 20 min observed from offline particle size measurements and at 10 min from FBRM data. It is believed that the delay in onset detection is caused by the fouling of the NIR probe window. A layer of fines was observed to have coated onto the window surface during the early stages of granulation. Though fouling also occurred on the FBRM probe, the problem may be more significant to NIR as it needs considerably more material to be near the probe window to give good measurements. Assuming that the layer of coated fines was removed by colliding granules after 50 min, the subsequent changes in absorbance from 80 to 130 min correlated well with the changes in particle size, which was in-line with previous studies (16,19).

Acoustic Emission Results

The average signal level (ASL) and counts per AE duration measured by R6I and R15I sensors are plotted in Figs. 8 and 9 respectively. As significant intensity was found to be around the average frequency of 50 kHz, sensor R6I with operating range from 40 to 100 kHz was more suitable for monitoring this process. Sensor R15I (70 to 200 kHz) did not detect significant signals during the first 14 min and the data collected was also more scattered as compared to those using R6I.

After the first 20 min, both ASL and counts per AE duration showed an increase corresponding to the onset of steady growth shown by the earlier reported particle size data. Throughout the subsequent granulation period, there was no significant change in acoustic data with accompanying changes in particle size except for an abrupt decline in counts from 80 to 100 min by sensor R15I. This showed that the onset of breakage or attrition as well as the drying phase during the last 10 min was not obvious from the AE data. The discontinuities in acoustic signals at regular time intervals at first 10 min and every subsequent 20 min can be attributed to the periodic increases and interruptions in fluidizing air flow rates (7). The adjustments in air flow rates were necessary to maintain the bed in a fluidized state due to the gradual increase in particle size. Due to the effect of air flow rate on the acoustic signals, it may be difficult to interpret whether changes in acoustic signals are caused by air flow or granule properties. In addition, as the piezoelectric sensors were very sensitive, any slight disturbance, such as an accidental tap on the granulator or heavy footsteps, would cause a temporary distortion in signals.

Two in-line (FBRM and NIR) and one non-intrusive (AE) PAT techniques have been applied to monitor granulation rate processes in a pilot-scale fluidized bed. In general, the PAT tools were able to detect the occurrence of the nucleation or induction, aggregation or steady-growth and breakage regimes, which were characterized from offline sample analyses using laser diffraction (PSD) and optical and scanning electron microscopy (morphology). The transition between induction and steady-growth phases corresponded well with an increase in FBRM chord length and acoustic average signal level as well as a decrease in FBRM chord count. Scattering of FBRM chord length distribution (CLD) data also disappeared once the fines have been agglomerated in the steady-growth regime. Fouling of the NIR probe window by the coating of fines seemed to have delayed the timely detection of this aggregation phase. When the breakage phase began, the particle size reduction corresponded with a decrease in FBRM chord length and NIR absorbance baseline as well as the re-emergence of CLD scattering. The onset of breakage did not give rise to significant changes in acoustic signals.

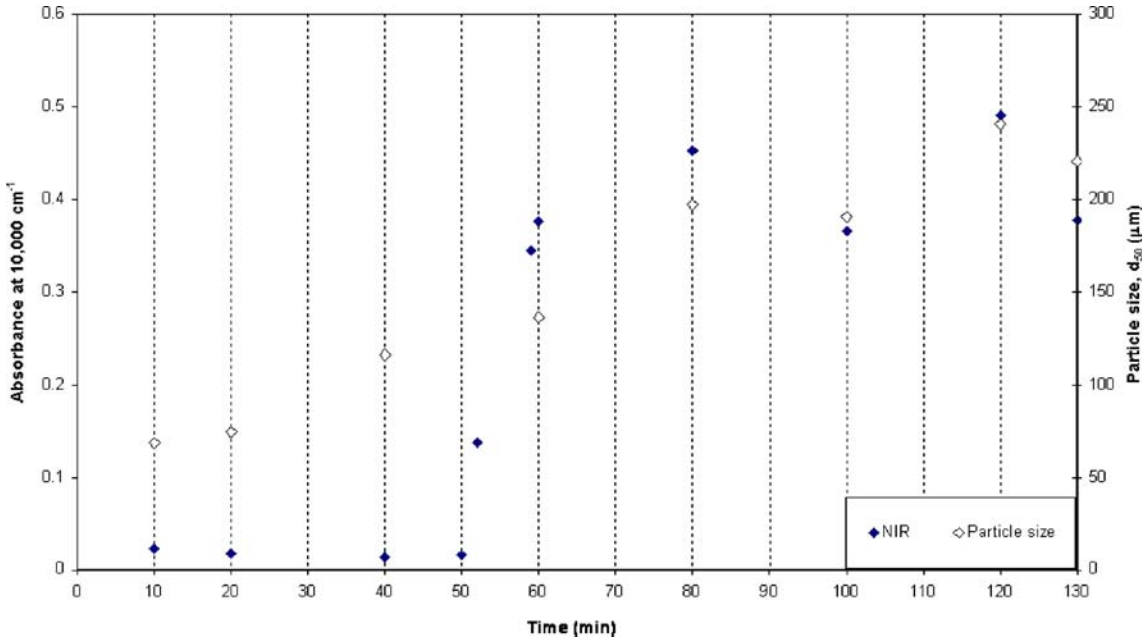

Fig. 7. NIR absorbance at wave number of 10,000 cm^{-1} and particle size against granulation time

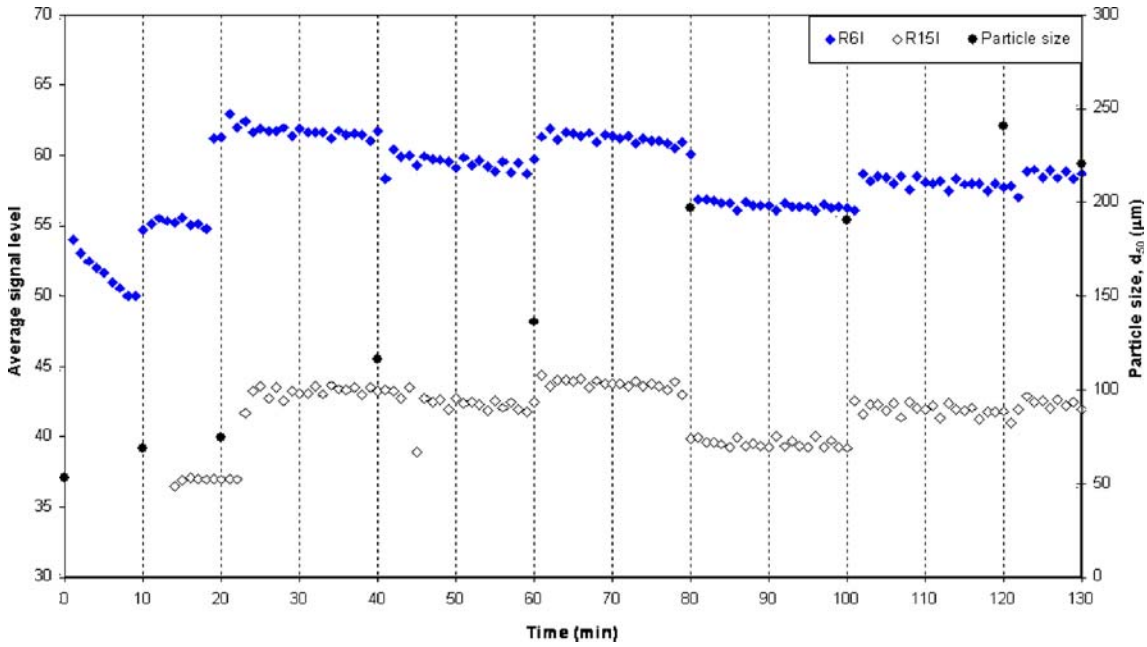

Fig. 8. AE average signal level for R6I and R15I

Comparing the three PAT techniques, as NIR and FBRM rely on high frequency waves to be transmitted and received through a transparent probe window, measurements can be obscured by the fouling of the probe windows. This problem could be potentially tackled by adding a heated purge air stream blown at the end of the probe to prevent sticking, which was devised by Watano (26). Another disadvantage of using the two intrusive probes is the interference with the fluidizing behavior inside the bed. As AE technique relies on detecting lower frequency signals, it has the advantage of not interfering with the fluidizing bed. However, in terms of sensitivity, it is affected by the background fluidizing air flow rates, material of construction, external unintended interferences, etc. It is the lowest cost option, which may be a useful technique to complement one of the optical methods, especially when the starting material is adhesive and prone to coating onto probe windows. In monitoring particle size, the FBRM is not affected by the influence of moisture content as compared to NIR and AE. Though not applied here, it is also important to note that a well working PAT system should be based on data analytic methods (i.e. chemometrics) to extract information, correlations and differences from the probe signals (27). Statistical treatment can be used to extract relevant information and reduce irrelevant information, i.e. interfering parameters (28).

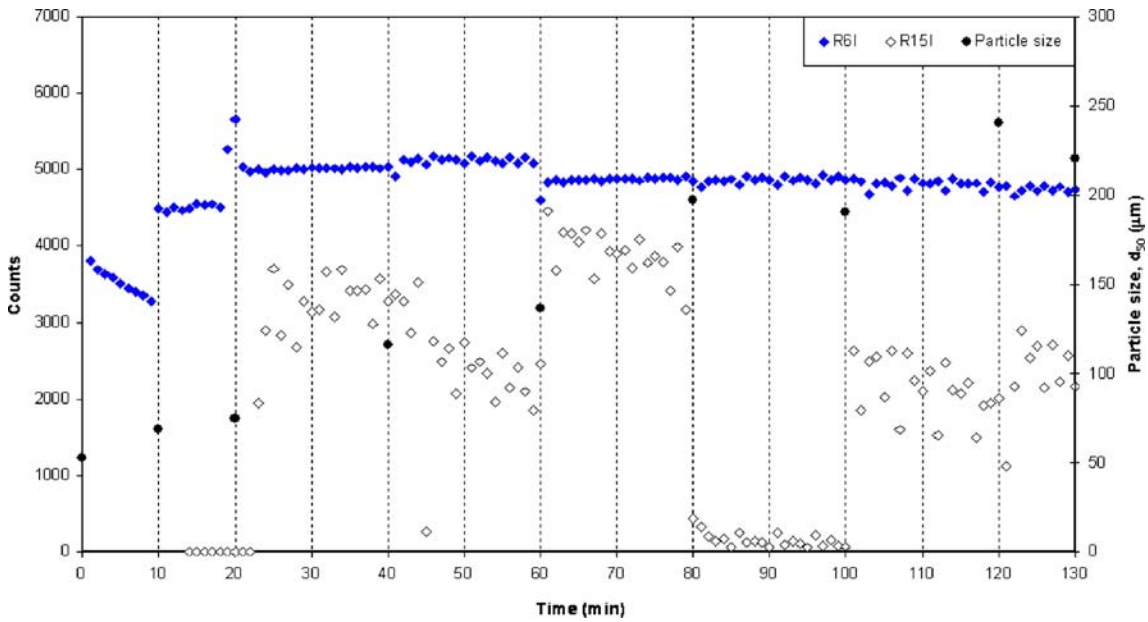

Fig. 9. AE counts chart for R6I and R15I

CONCLUSIONS

From an operational point of view, the three PAT techniques (FBRM, NIR and AE) were effective in monitoring whether a pilot-scale fluidized bed granulator was operating within a desired granulation rate process or regime, e.g., nucleation or steady-growth regime. The sensitivities, strengths and weaknesses of these techniques have been compared to facilitate the selection of suitable PAT tools for process design and scale-up. By coupling with scientific knowledge behind granulation rate processes, PAT techniques can potentially be used to develop a design space for a specific process and subsequently to detect any deviation from this space during operations.

ACKNOWLEDGMENT

This work was supported by the Science and Engineering Research Council of A*STAR (Agency for Science, Technology and Research).

REFERENCES

1. S. M. Iveson, P. A. L. Wauters, S. Forrest, J. D. Lister, G. M. H. Meesters, and B. Scarlett. Growth regime map for liquid-bound granules: further development and experimental validation. *Powder Technol.* **117**:83–97 (2001).
2. T. Lipsanen, O. Anitikaninen, H. Räikkönen, S. Airaksinen, and J. Ylirruusi. Novel description of a design space for fluidized bed granulation. *Int. J. Pharm.* **345**:101–107 (2007).
3. B. Rambali, L. Baert, and D. L. Massart. Scaling up of the fluidized bed granulation process. *Int. J. Pharm.* **252**:197–206 (2003).
4. M. Levin (Ed.). *Pharmaceutical process scale-up, 2nd edn.*, CRC, New York, 2006, pp. xii.
5. J. D. Cutnell, and W. J. Kenneth. *Physics*, 4th ed., Wiley, New York, 1998, p. 466.
6. M. Whitaker, G. R. Baker, J. Westrup, P. A. Goulding, D. R. Rudd, R. M. Belchamber, and P. C. Michael. Application of acoustic emission to the monitoring and end point determination of a high shear granulation process. *Int. J. Pharm.* **205**:79–91 (2000).
7. H. Tsujimoto, T. Yokoyama, C. C. Huang, and I. Sekiguchi. Monitoring particle fluidization in a fluidized bed granulator with an acoustic emission sensor. *Powder Technol.* **113**:88–96 (2000).
8. M. Halstensen, P. D. Bakker, and K. H. Esbensen. Acoustic chemometric monitoring of an industrial granulation production process—a PAT feasibility study. *Chemome. Intell. Lab. Syst.* **84**:88–97 (2006).
9. K. Naelapää, P. Veski, J. G. Pedersen, D. Anov, P. Jorgensen, H. G. Kristensen, and P. Bertelsen. Acoustic monitoring of a fluidized bed coating process. *Int. J. Pharm.* **332**:90–97 (2007).
10. S. Watano and K. Miyanami. Image processing for on-line monitoring of granule size distribution and shape in fluidized bed granulation. *Powder Technol.* **83**:55–60 (1995).
11. Z. Q. Yu, R. B. H. Tan, and P. S. Chow. Effects of operating conditions on agglomeration and habit of paracetamol crystals in anti-solvent crystallization. *J. Crystal Growth.* **279**:477–488 (2005).
12. M. Li, D. Wilkinson, and K. Patchigolla. Obtaining particle size distribution from chord length measurements. *Part. Part. Syst. Charact.* **23**:70–174 (2006).
13. J. Worlitschek and T. Hocker. Restoration of PSD from chord length distribution using the method of projects onto convex sets. *Part. Part. Syst. Charact.* **22**:81–98 (2005).
14. F. Sistare, L. S. P. Berry, and C. A. Mojica. Process Analytical Technology: an investment in process knowledge. *Organic Process Res. Dev.* **9**:332–336 (2005).
15. W. P. Findlay, R. P. Garnet, and K. R. Morris. Determination of fluidized bed granulation end point using near-infrared spectroscopy and phenomenological analysis. *J. Pharm. Sci.* **94**:604–612 (2005).
16. J. Rantanen, E. Rasanen, J. Tenhunen, M. Kansakoski, J.K. Mannermaa, and J. Yliruusi. In-line moisture measurement during granulation with a four-wavelength near infrared sensor: an evaluation of particle size and binder effects. *Eur. J. Pharm. Biopharm.* **50**:271–276 (2000).
17. J. Rantanen, S. Lehtola, P. Ramet, J. P. Mannermaa, and J. Yliruusi. On-line monitoring of moisture content in an instrumented fluidized bed granulator with a multi-channel NIR moisture sensor. *Powder Technol.* **99**:163–170 (1998).
18. P. Frake, D. Greenhalgh, S. M. Grierson, J. M. Hempenstall, and D. R. Rudd. Process control and end-point determination of a fluid bed granulation by application of near infra-red spectroscopy. *Int. J. Pharm.* **151**:75–80 (1997).
19. F. J. S. Nieuwmeyer, M. Damen, A. Gerich, F. Rusmini, K. V. D. V. Maarschalk, and H. Vromans. Granule characterization during fluid bed drying by development of a near infrared method to determine water content and median granule size. *Pharm. Res.* **24**:1854–1861 (2007). doi:10.1007/s11095-007-9305-5.
20. B. J. Ennis, and J. D. Litster. Particle size enlargement. In R. Perry, and D. Green (eds.), *Perry's Chemical Engineers' Handbook*, 7th edn, McGraw-Hill, New York, 1997, pp. 20–56, 20–89.
21. K. P. Hapgood, S. M. Iveson, J. D. Lister, and L. X. Liu. Granulation rate processes. In A.D. Salman, M. J. Hounslow, and J. P. K. Seville (eds.), *Handbook of powder technology, volume 11 Granulation*, Elsevier, Oxford, 2007, pp. 899, 934–935.
22. D. Geldart. Types of fluidization. *Powder Technol.* **7**:285, 1973 (1973).
23. D. KuniiO. Levenspiel. *Fluidization engineering*, Butterworth-Heinemann, Toronto, 1991.
24. A. R. Heath, P. D. Fawell, P. A. Bahri, and J. D. Swift. Estimating average particle size by focused beam reflectance measurement (FBRM). *Part. Part. Syst. Charact.* **19**:84–95 (2002).
25. J. Worlitschek and M. Mazzotti. Choice of the focal point position using Lasentec FBRM. *Part. Part. Syst. Charact.* **20**:12–17 (2002).
26. S. Watano. Direct control of wet granulation processes by image processing system. *Powder Technol.* **117**:163–172 (2001).
27. S. Wold, J. Cheney, N. Kettaneh, and C. McCready. The chemometric analysis of point and dynamic data in pharmaceutical and biotech production (PAT)—some objectives and approaches. *Chemome. Intell. Lab. Syst.* **84**:159–163 (2006).
28. G. Reich. Near-infrared spectroscopy and imaging: basic principles and pharmaceutical applications. *Adv. Drug Deliver. Rev.* **57**:1109–1143 (2005).